UPDATED PHOTOMETRY FOR THE KINGFISH SAMPLE OF NEARBY GALAXIES

D. A. Dale[1], M. Boquien[8], D. Calzetti[10], D. O. Cook[1], M. Galametz[12], K. D. Gordon[13], J. L. Hinz[3], L. K. Hunt[15], R. C. Kennicutt[12], H. Roussel[5], J. A. Turner[1], et al.

ABSTRACT

We present an update to the complete ultraviolet/optical/infrared/submillimeter/radio database of global photometry for the 79 nearby galaxies that comprise the union of the KINGFISH and SINGS samples. The dataset presented here includes contributions from *GALEX*, *SDSS*, *2MASS*, *WISE*, *Spitzer*, *Herschel*, *SCUBA*, and the *VLA*. Improvements of note include recalibrations of previously-published SINGS $BVR_{\rm C}I_{\rm C}$ and KINGFISH far-infrared/submillimeter photometry.

Subject headings: ISM: general — galaxies: ISM — infrared: ISM

1. Introduction

Access to a complete, panchromatic, photometric dataset is crucial to fully understanding the relative contributions to galaxy spectra from the various processes related to star formation and the accretion disks that feed supermassive black holes (Silva et al. 1998; da Cunha et al. 2008; Boquien 2016). Though a fairly complete multi-wavelength dataset has been published for the SINGS sample of 75 nearby galaxies (Kennicutt et al. 2003; Dale et al. 2005, 2007), subsequent far-infrared/submillimeter *Herschel* data were later published for the KINGFISH sample of nearby galaxies (Kennicutt et al. 2011; Dale et al. 2012), a sample for which 57 of the 61 targets are also SINGS targets. However, the calibration of a portion of the SINGS $BVR_{\rm C}I_{\rm C}$ from Dale et al. (2007) are suspect, and the calibration of the *Herschel* photometers have undergone multiple revisions since 2012.

In this effort we present an update to the global (spatially-integrated) photometry for the 79 nearby galaxies that comprise the union of the KINGFISH and SINGS samples. This update includes a Pan-STARRS1-based recalibration of previously-published $BVR_{\rm C}I_{\rm C}$ fluxes. In addition, the *Herschel* PACS photometry for NGC 0584 was not included in Dale et al.

[1]Department of Physics & Astronomy, University of Wyoming, Laramie, USA; ddale@uwyo.edu

(2012) since those imaging data were not yet taken. We also include new *ugriz* and 12 μm photometry respectively from the *Sloan Digital Sky Survey* (*SDSS*) and the *WISE* mission. Furthermore, we include new Herschel photometry for six SINGS galaxies from the Herschel Very Nearby Galaxy Survey (PI C. Wilson) that are not in the KINGFISH sample (N2403, M81=NGC 3031, M82=NGC 3034, N4125, M51a=NGC 5194, and M51b=NGC 5195). Finally, we complete the presentation of a multi-wavelength database by including previously published global photometry from ultraviolet (*GALEX*), infrared (*2MASS*, *Spitzer*), and radio (VLA) wavelengths.

2. Observations and Data Processing

2.1. Optical

SDSS ugriz imaging (Data Release) was used to provide optical fluxes for 51 of the 79 galaxies. $BVR_{\rm C}I_{\rm C}$ photometry for 57 galaxies was re-estimated from a recalibration of the SINGS data originally published in Dale et al. (2007). The union of the *SDSS ugriz* and recalibrated $BVR_{\rm C}I_{\rm C}$ samples comprises 63 galaxies, and thus for 80% of the sample we have reliable optical photometry. This fraction approaches 100% after inclusion of $BVR_{\rm C}I_{\rm C}$ photometry from other global photometric datasets (de Vaucouleurs et al. 1991; Muñoz-Mateos et al. 2009; Tully et al. 2009; Cook et al. 2014).

The recalibration of the $BVR_{\rm C}I_{\rm C}$ fluxes was carried out via comparison of photometry on foreground stars in Pan-STARRS1 $u_{\rm PS1}g_{\rm PS1}r_{\rm PS1}z_{\rm PS1}$ and our 2007-era $BVR_{\rm C}I_{\rm C}$ imaging. We adopted the quadratic filter transformations of Tonry et al. (2012) between Pan-STARRS1 $u_{\rm PS1}g_{\rm PS1}r_{\rm PS1}z_{\rm PS1}$ and $BVR_{\rm C}I_{\rm C}$, though very similar results are obtained when using transformations between *SDSS* and Johnson/Cousins filters.

New editing of foreground stars and background galaxies

New definitions of sky regions (larger and more representative)

Slightly updated optical data processing (less striping in n0628, e.g.)

Table 1. Galaxy Sample

Galaxy	Alternative Name	Optical Morph.	$E(B-V)$ (mag.)	α_0 & δ_0 (J2000)	$2a$ ($''$)	$2b$ ($''$)	PA ($^\circ$)	D_{25} (Mpc)	TIR ($L_\odot$)
NGC0024	UGCA002	SAc	0.017	000955.9−245755	301	216	45	8.20	8.8
NGC0337	NGC0337	SBd	0.096	005950.7−073444	253	194	140	19.30	10.1
NGC0584	NGC0584	E4	0.036	013120.6−065205	326	278	60	20.80	8.8
NGC0628	M074	SAc	0.060	013642.4+154711	879	808	90	7.20	9.9
NGC0855	UGC01718	E	0.061	021403.7+275237	259	169	60	9.73	8.6
NGC0925	UGC01913	SABd	0.065	022713.6+333504	735	486	105	9.12	9.7
NGC1097	UGCA041	SBb	0.023	024618.0−301642	758	612	130	14.20	10.6
NGC1266	NGC1266	SB0	0.085	031600.6−022541	234	232	0	30.60	10.4
NGC1291	NGC1291	SB0/a	0.011	031717.9−410616	884	836	90	10.40	9.5
NGC1316	FornaxA	SAB0	0.018	032241.2−371210	864	583	50	21.00	9.9
NGC1377	NGC1377	S0	0.024	033639.0−205408	181	162	90	24.60	10.1
NGC1404	NGC1404	E1	0.010	033852.3−353540	524	369	149	20.20	···
IC0342	UGC02847	SABcd	0.480	034659.5+680539	1667	1439	100	3.28	10.1
NGC1482	NGC1482	SA0	0.034	035439.0−203009	349	310	119	22.60	10.6
NGC1512	NGC1512	SBab	0.009	040355.6−432149	1001	928	83	11.60	9.5
NGC1566		SABbc	0.008	042000.4−545615	552	435	40	18.00	10.6
NGC1705		SA0	0.007	045413.5−532137	167	120	40	5.80	8.0
NGC2146	UGC03429	Sbab	0.082	061835.6+782129	236	235	120	17.20	11.1
NGC2403	UGC03918	SABcd	0.034	073655.1+653534	1512	929	124	3.50	9.6
HolmbergII	UGC04305	Im	0.027	081910.8+704320	554	465	60	3.05	7.8
M081DwarfA		I?	0.018	082356.0+710145	78	78	90	3.50	···
DDO053	UGC04459	Im	0.033	083407.4+661043	155	142	90	3.61	7.0
NGC2798	UGC04905	SBa	0.017	091723.1+415957	235	232	90	25.80	10.6
NGC2841	UGC04966	SAb	0.013	092203.3+505837	629	334	150	14.10	10.1
NGC2915		I0	0.236	092609.4−763736	183	132	110	3.78	7.6
HolmbergI	UGC05139	IABm	0.044	094033.6+711120	264	219	63	3.90	7.1
NGC2976	UGC05221	SAc	0.062	094715.3+675509	541	353	144	3.55	8.9
NGC3049	UGC05325	SBab	0.033	095449.6+091614	218	160	29	19.20	9.5
NGC3031	M081	SAab	0.069	095531.8+690403	1628	1122	154	3.50	9.6
NGC3034	M082	I0	0.134	095552.1+694057	698	581	65	3.50	10.7
HolmbergIX	UGC05336	Im	0.068	095729.2+690250	247	180	40	3.50	···
NGC3077	UGC05398	I0pec	0.058	100317.5+684354	488	436	64	3.83	8.9
M081DwarfB	UGC05423	Im	0.068	100531.2+702151	134	90	139	3.60	6.5
NGC3190	UGC05559	SAap	0.022	101805.7+214957	334	196	117	19.30	9.8
NGC3184	UGC05557	SABcd	0.014	101815.6+412542	614	538	169	11.70	10.0
NGC3198	UGC05572	SBc	0.011	101954.8+453301	518	315	35	14.10	10.0
IC2574	UGC05666	SABm	0.031	102823.9+682505	864	486	59	3.79	8.3
NGC3265	UGC05705	E	0.021	103106.8+284751	184	175	50	19.60	9.4
Mrk33	UGC05720	Im	0.010	103231.2+542359	181	177	90	21.70	9.8
NGC3351	M095	SBb	0.024	104358.1+114210	592	441	11	9.33	9.9
NGC3521	UGC06150	SABbc	0.049	110548.1−000127	926	455	165	11.20	10.5
NGC3621	UGCA232	SAd	0.069	111818.3−324855	791	555	160	6.55	9.9
NGC3627	M066	SABb	0.029	112013.4+125927	745	486	167	9.38	10.4
NGC3773	UGC06605	SA0	0.023	113813.1+120644	118	116	0	12.40	8.8
NGC3938	UGC06856	SAc	0.018	115250.3+440715	504	468	0	17.90	10.3

Table 1—Continued

Galaxy	Alternative Name	Optical Morph.	$E(B-V)$ (mag.)	α_0 & δ_0 (J2000)	$2a$ ($''$)	$2b$ ($''$)	PA ($^\circ$)	D_{25} (Mpc)	TIR ($L_\odot$)
NGC4125	UGC07118	E6p	0.016	120805.8+651024	228	151	90	21.40	9.1
NGC4236	UGC07306	SBdm	0.013	121643.2+692719	1240	369	162	4.45	8.7
NGC4254	M099	SAc	0.033	121849.7+142519	519	420	60	14.40	10.6
NGC4321	M100	SABbc	0.023	122254.8+154907	558	483	40	14.30	10.5
NGC4450	UGC07594	SAab	0.024	122830.1+170454	401	284	180	20.00	9.9
NGC4536	UGC07732	SABbc	0.016	123427.5+021113	454	376	120	14.50	10.3
NGC4552	M089	E	0.035	123539.8+123323	306	306	90	4.90	7.7
NGC4559	UGC07766	SABcd	0.015	123558.1+275752	576	327	140	6.98	9.5
NGC4569	M090	SABab	0.040	123650.2+131001	593	327	21	9.86	9.7
NGC4579	M058	SABb	0.035	123743.8+114858	325	271	90	16.40	10.1
NGC4594	M104	SAa	0.044	123959.6−113726	767	669	90	9.08	9.6
NGC4625	UGC07861	SABmp	0.016	124154.8+411623	298	214	100	9.30	8.8
NGC4631	UGC07865	SBd	0.015	124204.2+323219	901	240	85	7.62	10.4
NGC4725	UGC07989	SABab	0.010	125027.7+252948	689	523	30	11.90	9.9
NGC4736	M094	SAab	0.015	125055.2+410652	944	899	0	4.66	9.8
DDO154	UGC08024	IBm	0.008	125407.6+270916	216	126	50	4.30	···
NGC4826	M064	SAab	0.036	125643.3+214048	716	427	114	5.27	9.6
DDO165	UGC08201	Im	0.021	130625.9+674229	263	161	90	4.57	···
NGC5033	UGC08307	SAc	0.010	131328.2+363534	729	467	180	13.30	10.3
NGC5055	M063	SAbc	0.015	131549.2+420147	1097	711	80	7.94	10.3
NGC5194	M051a	SABbc	0.030	132950.6+471307	1699	1129	15	8.20	10.6
NGC5195	M051b	SB0p	0.031	132959.4+471556	202	191	0	8.20	9.3
NGC5398	Tololo89	SBdm	0.056	140121.2−330402	198	146	0	7.66	8.6
NGC5457	M101	SABcd	0.007	140325.0+542429	1800	1446	37	6.70	10.3
NGC5408		IBm	0.059	140321.1−412241	256	209	67	4.80	8.3
NGC5474	UGC09013	SAcd	0.009	140500.8+533920	412	373	90	6.80	8.7
NGC5713	UGC09451	SABbcp	0.034	144011.4−001726	225	225	90	21.37	10.5
NGC5866	UGC09723	S0	0.012	150628.8+554551	500	306	129	15.30	9.7
IC4710		SBm	0.076	182838.9−665903	313	219	120	8.50	8.6
NGC6822	DDO229	IBm	0.199	194453.2−144811	1453	1100	150	0.60	7.8
NGC6946	UGC11597	SABcd	0.294	203449.2+600959	953	928	0	6.80	10.5
NGC7331	UGC12113	SAb	0.078	223704.3+342435	683	335	168	14.50	10.7
NGC7552	IC5294	SAc	0.012	231610.8−423505	441	325	120	22.30	11.0
NGC7793		SAd	0.017	235749.9−323525	716	526	98	3.91	9.3

Note. — $2a$ and $2b$ are the lengths of the major and minor axes used in the elliptical aperture photometry described herein; the position angle of the aperture's major axis is measured east of north. The total infrared luminosity listed in the last column is derived from Equation 5 of Dale et al. (2014) and the 8, 24, 70, and 160 μm fluxes in 2c and assumes the distances provided in this table.

Table 2a. Global Flux Densities in Janskys

Galaxy	FUV	NUV	B	V	R_C	I_C	u	g	r	i
$\lambda(\mu m)$	0.1528	0.2271	0.440	0.553	0.640	0.790	0.3557	0.4825	0.6261	0.7672
A_λ/A_V	2.586	2.994	1.3103	1.0	0.7884	0.5766	1.6415	1.2190	0.8487	0.6405
NGC0024	874±137E−3	113±017E−2	870±022E−2	113±002E−1	143±007E−1	188±008E−1	···	···	···	···
NGC0337	943±130E−3	186±025E−2	112±006E−1	119±005E−1	134±007E−1	162±018E−1	389±009E−2	928±019E−2	126±002E−1	144±003E−1
NGC0584	360±051E−4	200±027E−3	149±017E−1	293±023E−1	376±042E−1	551±051E−1	347±008E−2	163±003E−1	323±006E−1	462±009E−1
NGC0628	733±115E−2	990±152E−2	661±041E−1	141±006E+0	140±006E+0	216±012E+0	238±004E−1	608±012E−1	930±018E−1	120±002E+0
NGC0855	144±022E−3	301±046E−3	256±025E−2	399±039E−2	524±014E−2	···	110±003E−2	331±007E−2	542±011E−2	709±015E−2
NGC0925	475±065E−2	624±086E−2	339±017E−1	549±149E−1	538±045E−1	669±055E−1	···	···	···	···
NGC1097	353±050E−2	509±071E−2	406±014E−1	684±025E−1	945±034E−1	129±004E+0	···	···	···	···
NGC1266	045±006E−4	291±041E−4	200±013E−2	368±019E−2	488±037E−2	733±054E−2	···	···	···	···
NGC1291	757±118E−3	166±025E−2	604±022E−1	122±004E+0	176±006E+0	245±009E+0	···	···	···	···
NGC1316	307±042E−3	165±022E−2	837±030E−1	164±006E+0	235±008E+0	299±011E+0	···	···	···	···
NGC1377	···	···	230±012E−2	375±015E−2	478±033E−2	761±023E−2	···	···	···	···
NGC1404	956±132E−4	276±038E−3	178±006E−1	365±013E−1	525±019E−1	776±028E−1	···	···	···	···
IC0342	···	···	588±080E+0	···	···	···	···	···	···	···
NGC1482	391±061E−4	143±020E−3	567±031E−2	763±049E−2	105±010E−1	159±013E−1	···	···	···	···
NGC1512	169±026E−2	179±030E−2	151±005E−1	259±009E−1	359±013E−1	496±018E−1	···	···	···	···
NGC1566	540±075E−2	654±090E−2	359±013E−1	607±022E−1	709±026E−1	875±032E−1	···	···	···	···
NGC1705	166±026E−2	157±024E−2	274±010E−2	373±013E−2	406±014E−2	543±020E−2	···	···	···	···
NGC2146	···	···	163±020E−1	266±034E−1	···	615±017E−1	···	···	···	···
NGC2403	238±038E−1	296±045E−1	147±014E+0	227±032E+0	245±009E+0	318±008E+0	734±025E−1	170±005E+0	240±008E+0	296±010E+0
HoII	416±065E−2	467±071E−2	140±010E−1	161±007E−1	214±024E−1	316±051E−1	···	···	···	···
M81dwA	476±065E−4	567±078E−4	107±043E−3	950±420E−4	114±042E−3	144±062E−3	···	···	···	···
DDO053	273±042E−3	273±042E−3	746±181E−3	900±220E−3	592±194E−3	844±274E−3	296±017E−3	578±020E−3	649±022E−3	669±024E−3
NGC2798	109±015E−3	233±032E−3	317±028E−2	572±034E−2	670±034E−2	113±010E−1	907±030E−3	330±007E−2	623±013E−2	853±018E−2
NGC2841	128±017E−2	206±028E−2	458±021E−1	794±028E−1	104±007E+0	180±010E+0	118±002E−1	480±009E−1	972±019E−1	143±002E+0
NGC2915	124±017E−2	163±022E−2	517±051E−2	605±022E−2	865±031E−2	737±073E−2	···	···	···	···
HoI	510±080E−3	583±088E−3	136±034E−2	173±043E−2	162±047E−2	226±056E−2	···	···	···	···
NGC2976	198±031E−2	295±045E−2	278±018E−1	426±013E−1	533±034E−1	748±050E−1	100±002E−1	279±005E−1	465±009E−1	603±012E−1
NGC3049	···	449±062E−3	278±022E−2	394±019E−2	427±030E−2	561±053E−2	108±003E−2	263±006E−2	423±009E−2	531±011E−2
NGC3031	167±026E−1	239±036E−1	384±038E+0	742±074E+0	···	158±004E+1	128±004E+0	483±016E+0	930±031E+0	135±004E+1
NGC3034	274±043E−2	909±138E−2	183±030E+0	241±024E+0	330±044E+0	470±056E+0	639±021E−1	168±005E+0	323±011E+0	439±014E+0
HoIX	372±051E−3	499±069E−3	734±116E−3	667±133E−3	687±140E−3	100±033E−2	508±027E−3	100±003E−2	107±003E−2	125±004E−2
NGC3077	···	···	227±006E−1	···	614±016E−1	···	913±020E−2	323±006E−1	571±011E−1	764±015E−1
M81dwB	778±122E−4	105±016E−3	620±207E−3	790±255E−3	933±315E−3	929±257E−3	249±017E−3	572±020E−3	817±026E−3	962±029E−3

Table 2a—Continued

Galaxy	FUV	NUV	B	V	R_C	I_C	u	g	r	i
$\lambda(\mu m)$	0.1528	0.2271	0.440	0.553	0.640	0.790	0.3557	0.4825	0.6261	0.7672
A_λ/A_V	2.586	2.994	1.3103	1.0	0.7884	0.5766	1.6415	1.2190	0.8487	0.6405
NGC3190	392±054E−4	180±024E−3	108±004E−1	192±005E−1	266±008E−1	415±016E−1	240±006E−2	110±002E−1	222±004E−1	330±006E−1
NGC3184	415±057E−2	556±077E−2	354±030E−1	498±021E−1	584±040E−1	757±042E−1	114±002E−1	333±006E−1	527±010E−1	685±013E−1
NGC3198	233±032E−2	284±039E−2	208±008E−1	259±013E−1	303±024E−1	405±033E−1	662±014E−2	178±003E−1	278±005E−1	357±007E−1
IC2574	491±077E−2	529±080E−2	157±021E−1	201±027E−1	195±031E−1	278±037E−1	···	···	···	···
NGC3265	552±076E−4	963±133E−4	121±015E−2	180±008E−2	228±021E−2	364±052E−2	399±019E−3	122±003E−2	219±005E−2	300±007E−2
Mrk33	407±056E−3	518±071E−3	203±014E−2	291±056E−2	343±074E−2	398±079E−2	···	···	···	···
NGC3351	175±027E−2	296±045E−2	330±041E−1	570±041E−1	738±053E−1	112±006E+0	980±021E−2	356±007E−1	657±013E−1	917±018E−1
NGC3521	208±033E−2	452±069E−2	756±029E−1	124±002E+0	164±002E+0	244±007E+0	214±004E−1	788±015E−1	145±002E+0	198±003E+0
NGC3621	714±104E−2	110±015E−1	555±020E−1	795±029E−1	912±033E−1	116±004E+0	···	···	···	···
NGC3627	304±047E−2	578±088E−2	826±047E−1	125±002E+0	150±013E+0	226±012E+0	245±005E−1	840±016E−1	146±002E+0	201±004E+0
NGC3773	410±056E−3	554±076E−3	181±009E−2	241±008E−2	272±022E−2	339±027E−2	848±027E−3	177±004E−2	268±006E−2	321±007E−2
NGC3938	···	363±050E−2	234±009E−1	324±006E−1	361±020E−1	501±017E−1	786±017E−2	217±004E−1	328±006E−1	421±008E−1
NGC4125	···	343±047E−3	215±003E−1	387±007E−1	523±012E−1	784±050E−1	···	···	···	···
NGC4236	685±107E−2	828±126E−2	359±031E−1	409±032E−1	493±039E−1	572±055E−1	···	···	···	···
NGC4254	···	618±085E−2	390±024E−1	535±016E−1	662±024E−1	808±027E−1	149±003E−1	381±007E−1	588±011E−1	741±014E−1
NGC4321	···	539±074E−2	481±022E−1	715±019E−1	936±044E−1	137±008E+0	169±003E−1	477±009E−1	797±016E−1	107±002E+0
NGC4450	···	538±074E−3	220±011E−1	394±011E−1	533±018E−1	799±033E−1	···	···	···	···
NGC4536	166±023E−2	219±030E−2	196±013E−1	285±024E−1	355±036E−1	534±103E−1	610±013E−2	181±003E−1	304±006E−1	405±008E−1
NGC4552	181±025E−3	464±064E−3	262±011E−1	470±011E−1	653±017E−1	998±054E−1	···	···	···	···
NGC4559	529±073E−2	646±089E−2	323±021E−1	414±012E−1	467±034E−1	584±041E−1	117±002E−1	292±005E−1	417±008E−1	516±010E−1
NGC4569	575±079E−3	196±027E−2	389±038E−1	623±062E−1	···	···	110±002E−1	415±008E−1	687±013E−1	969±019E−1
NGC4579	563±077E−3	120±016E−2	334±013E−1	591±023E−1	751±047E−1	111±006E+0	780±016E−2	338±006E−1	655±013E−1	941±018E−1
NGC4594	520±081E−3	162±025E−2	122±007E+0	274±036E+0	323±010E+0	487±030E+0	298±006E−1	144±002E+0	295±005E+0	435±008E+0
NGC4625	617±098E−3	799±123E−3	386±029E−2	551±049E−2	639±089E−2	826±059E−2	135±004E−2	360±008E−2	555±012E−2	707±015E−2
NGC4631	107±016E−1	133±020E−1	650±051E−1	847±032E−1	976±049E−1	122±005E+0	268±005E−1	609±012E−1	886±017E−1	111±002E+0
NGC4725	218±030E−2	296±041E−2	484±025E−1	850±022E−1	107±003E+0	166±007E+0	129±002E−1	496±010E−1	932±018E−1	134±002E+0
NGC4736	699±109E−2	922±140E−2	149±009E+0	225±006E+0	302±010E+0	442±024E+0	442±008E−1	170±003E+0	311±006E+0	433±008E+0
DDO154	438±068E−3	430±066E−3	108±029E−2	115±035E−2	123±030E−2	128±032E−2	473±020E−3	908±026E−3	103±003E−2	103±003E−2
NGC4826	130±020E−2	350±053E−2	109±009E+0	165±009E+0	206±019E+0	321±018E+0	269±005E−1	109±002E+0	201±004E+0	286±005E+0
DDO165	562±088E−3	787±120E−3	307±076E−2	293±029E−2	266±057E−2	350±129E−2	101±003E−2	236±005E−2	269±006E−2	296±007E−2
NGC5033	195±027E−2	256±035E−2	250±012E−1	403±022E−1	···	646±042E−1	···	···	···	···
NGC5055	413±064E−2	666±103E−2	850±085E−1	138±013E+0	188±005E+0	281±007E+0	302±006E−1	984±019E−1	177±003E+0	252±005E+0
NGC5194	134±021E−1	214±032E−1	149±017E+0	199±013E+0	230±022E+0	340±030E+0	551±018E−1	136±004E+0	218±007E+0	280±009E+0

Table 2a—Continued

Galaxy	FUV	NUV	B	V	R_C	I_C	u	g	r	i
$\lambda(\mu m)$	0.1528	0.2271	0.440	0.553	0.640	0.790	0.3557	0.4825	0.6261	0.7672
A_λ/A_V	2.586	2.994	1.3103	1.0	0.7884	0.5766	1.6415	1.2190	0.8487	0.6405
NGC5195	195±031E−3	546±085E−3	419±048E−1	668±045E−1	863±082E−1	157±014E+0	136±004E−1	396±013E−1	773±026E−1	109±003E+0
NGC5398	712±098E−3	113±015E−2	594±059E−2	594±059E−2	457±045E−2	570±057E−2	···	···	···	···
NGC5457	369±***E−4	432±***E−4	207±017E+0	266±025E+0	290±008E+0	436±012E+0	781±015E−1	194±003E+0	280±005E+0	356±007E+0
NGC5408	···	···	700±070E−2	950±095E−2	···	···	···	···	···	···
NGC5474	247±038E−2	271±041E−2	128±007E−1	169±006E−1	183±012E−1	218±019E−1	511±011E−2	120±002E−1	170±003E−1	202±004E−1
NGC5713	497±068E−3	100±013E−2	104±007E−1	147±006E−1	188±006E−1	251±026E−1	335±007E−2	993±020E−2	164±003E−1	209±004E−1
NGC5866	636±088E−4	414±057E−3	245±011E−1	443±016E−1	556±038E−1	865±050E−1	583±012E−2	265±005E−1	506±010E−1	746±015E−1
IC4710	207±028E−2	301±041E−2	753±075E−2	991±099E−2	835±083E−2	···	···	···	···	···
NGC6822	249±034E−1	405±056E−1	138±007E+0	882±045E−1	190±006E+0	213±017E+0	···	···	···	···
NGC6946	161±022E−1	415±057E−1	183±018E+0	296±013E+0	···	567±055E+0	···	···	···	···
NGC7331	143±019E−2	296±041E−2	607±034E−1	894±017E−1	121±003E+0	191±008E+0	130±002E−1	507±010E−1	984±019E−1	143±002E+0
NGC7552	763±105E−3	151±021E−2	133±004E−1	224±008E−1	232±023E−1	218±021E−1	···	···	···	···
NGC7793	126±019E−1	149±022E−1	586±058E−1	803±080E−1	774±077E−1	680±068E−1	···	···	···	···

Note. — The compact table entry format TUV±WXYEZ implies (T.UV±W.XY)×10^Z in Jy. See § 2 for corrections that have been applied to the data. The uncertainties include both statistical and systematic effects. 5σ upper limits are provided for non-detections. No color corrections have been applied.

Table 2b. Global Flux Densities in Janskys

Galaxy	z	J	H	K_s	IRAC	IRAC	IRAC	IRAC	WISE	MIPS
$\lambda(\mu m)$	0.9097	1.25	1.65	2.17	3.6	4.5	5.8	8.0	12	24
A_λ/A_V	0.4882	0.2964	0.1871	0.1159	0.04514	0.02880	0.01930	0.02962	0.03554	0.01932
NGC0024	···	231±012E−1	248±013E−1	189±012E−1	101±013E−1	683±101E−2	822±116E−2	117±016E−1	952±095E−2	120±012E−1
NGC0337	156±003E−1	193±019E−1	200±020E−1	170±017E−1	970±128E−2	665±091E−2	141±018E−1	379±047E−1	302±030E−1	677±028E−1
NGC0584	593±012E−1	908±090E−1	111±011E+0	870±087E−1	367±049E−1	219±029E−1	174±022E−1	114±014E−1	723±072E−2	481±020E−2
NGC0628	134±002E+0	164±008E+0	166±008E+0	131±007E+0	846±118E−1	546±075E−1	116±014E+0	260±033E+0	243±024E+0	324±034E+0
NGC0855	832±018E−2	898±054E−2	972±066E−2	794±067E−2	431±060E−2	281±039E−2	360±030E−2	476±057E−2	366±036E−2	854±092E−2
NGC0925	···	593±059E−1	643±064E−1	511±051E−1	310±042E−1	211±028E−1	350±044E−1	609±076E−1	564±056E−1	946±040E−1
NGC1097	···	239±023E+0	273±027E+0	228±022E+0	124±016E+0	801±109E−1	146±018E+0	318±039E+0	307±030E+0	662±027E+0
NGC1266	···	121±012E−1	126±012E−1	119±011E−1	544±074E−2	417±054E−2	545±073E−2	885±112E−2	115±011E−1	876±036E−1
NGC1291	···	436±021E+0	455±022E+0	398±020E+0	208±028E+0	127±017E+0	906±122E−1	639±079E−1	610±061E−1	481±051E−1
NGC1316	···	468±046E+0	489±048E+0	420±042E+0	248±033E+0	153±021E+0	112±014E+0	553±069E−1	623±062E−1	428±021E−1
NGC1377	···	100±010E−1	114±011E−1	944±094E−2	568±075E−2	851±117E−2	267±035E−1	420±052E−1	410±041E−1	183±007E+0
NGC1404	···	137±013E+0	159±015E+0	134±013E+0	728±098E−1	434±059E−1	331±042E−1	158±019E−1	141±014E−1	880±040E−2
IC0342	···	143±007E+1	137±006E+1	126±006E+1	142±019E+1	819±112E+0	130±016E+1	283±035E+1	252±025E+1	372±014E+1
NGC1482	···	232±023E−1	300±030E−1	293±029E−1	205±028E−1	151±020E−1	593±076E−1	155±019E+0	127±012E+0	368±014E+0
NGC1512	···	810±043E−1	855±048E−1	729±046E−1	439±052E−1	294±033E−1	260±034E−1	456±054E−1	437±043E−1	486±052E−1
NGC1566	···	138±013E+0	141±014E+0	126±012E+0	750±101E−1	479±065E−1	907±115E−1	211±026E+0	194±019E+0	283±012E+0
NGC1705	···	573±036E−2	539±044E−2	443±047E−2	266±036E−2	193±025E−2	183±019E−2	192±020E−2	200±020E−2	538±058E−2
NGC2146	···	956±048E−1	122±006E+0	110±005E+0	844±114E−1	634±087E−1	251±032E+0	681±085E+0	513±051E+0	124±004E+1
NGC2403	322±011E+0	292±014E+0	290±014E+0	238±012E+0	200±025E+0	135±017E+0	211±026E+0	387±051E+0	407±040E+0	588±063E+0
HoII	···	165±011E−1	290±019E−1	215±018E−1	774±098E−2	645±078E−2	400±047E−2	441±048E−2	430±043E−2	177±019E−1
M81dwA	···	376±038E−3	388±038E−3	292±029E−3	185±094E−3	960±960E−4	<376E−3	<236E−3	<630E−4	<173E−2
DDO053	633±043E−3	750±206E−3	137±031E−2	792±370E−3	427±100E−3	310±100E−3	264±090E−3	438±100E−3	662±068E−3	240±026E−2
NGC2798	108±002E−1	162±016E−1	185±018E−1	173±017E−1	114±015E−1	811±114E−2	265±034E−1	633±079E−1	605±060E−1	262±010E+0
NGC2841	182±003E+0	280±028E+0	321±032E+0	266±026E+0	127±017E+0	751±103E−1	669±085E−1	115±014E+0	103±010E+0	909±037E−1
NGC2915	···	125±012E−1	145±014E−1	907±090E−2	537±075E−2	347±050E−2	326±044E−2	310±039E−2	190±019E−2	628±026E−2
HoI	···	307±043E−2	395±063E−2	159±073E−2	964±141E−3	597±120E−3	374±180E−3	363±161E−3	169±084E−3	656±098E−3
NGC2976	705±014E−1	851±043E−1	887±045E−1	704±037E−1	408±059E−1	283±039E−1	515±065E−1	102±012E+0	864±086E−1	139±015E+0
NGC3049	627±014E−2	773±077E−2	816±081E−2	737±073E−2	403±052E−2	274±038E−2	652±086E−2	134±017E−1	115±011E−1	427±017E−1
NGC3031	174±005E+1	232±011E+1	252±012E+1	211±010E+1	106±014E+1	655±090E+0	558±074E+0	764±100E+0	600±060E+0	523±056E+0
NGC3034	546±018E+0	908±045E+0	106±005E+1	100±005E+1	725±227E+0	573±180E+0	236±073E+1	620±191E+1	<351E+1	324±102E+2
HoIX	141±006E−2	244±024E−2	203±020E−2	146±014E−2	736±114E−3	379±036E−3	<131E−2	<119E−2	<544E−3	<364E−2
NGC3077	890±017E−1	104±005E+0	103±005E+0	866±045E−1	537±072E−1	361±049E−1	432±054E−1	812±101E−1	773±077E−1	130±014E+0
M81dwB	110±004E−2	118±015E−2	135±022E−2	135±027E−2	539±101E−3	362±101E−3	322±090E−3	309±080E−3	387±***E−3	333±047E−3

Table 2b—Continued

Galaxy	z	J	H	K_s	IRAC	IRAC	IRAC	IRAC	WISE	MIPS
$\lambda(\mu m)$	0.9097	1.25	1.65	2.17	3.6	4.5	5.8	8.0	12	24
A_λ/A_V	0.4882	0.2964	0.1871	0.1159	0.04514	0.02880	0.01930	0.02962	0.03554	0.01932
NGC3190	437±008E−1	710±071E−1	833±083E−1	739±073E−1	372±050E−1	234±032E−1	247±031E−1	328±041E−1	286±028E−1	266±011E−1
NGC3184	769±015E−1	104±010E+0	113±011E+0	912±091E−1	557±075E−1	356±049E−1	666±084E−1	143±017E+0	119±011E+0	142±005E+0
NGC3198	424±008E−1	573±057E−1	631±063E−1	547±054E−1	273±037E−1	173±023E−1	335±042E−1	683±085E−1	623±062E−1	105±004E+0
IC2574	···	334±019E−1	230±019E−1	164±021E−1	148±020E−1	110±012E−1	643±087E−2	690±089E−2	456±046E−2	281±030E−1
NGC3265	367±009E−2	506±050E−2	572±057E−2	479±047E−2	284±037E−2	198±026E−2	411±054E−2	101±012E−1	881±088E−2	295±012E−1
Mrk33	···	490±049E−2	558±055E−2	477±047E−2	265±036E−2	189±026E−2	528±067E−2	127±016E−1	161±016E−1	862±035E−1
NGC3351	114±002E+0	167±008E+0	176±008E+0	153±007E+0	772±110E−1	501±071E−1	659±092E−1	127±016E+0	119±011E+0	253±027E+0
NGC3521	252±005E+0	370±018E+0	419±021E+0	348±017E+0	196±027E+0	129±018E+0	236±032E+0	561±076E+0	499±049E+0	549±059E+0
NGC3621	···	192±019E+0	213±021E+0	168±016E+0	992±134E−1	668±091E−1	160±020E+0	349±043E+0	304±030E+0	369±018E+0
NGC3627	245±004E+0	332±016E+0	372±018E+0	316±015E+0	178±025E+0	115±017E+0	219±030E+0	522±069E+0	475±047E+0	752±029E+0
NGC3773	357±008E−2	451±045E−2	385±038E−2	373±037E−2	222±027E−2	143±016E−2	255±034E−2	475±059E−2	421±042E−2	144±005E−1
NGC3938	476±009E−1	635±063E−1	575±057E−1	534±053E−1	321±043E−1	211±029E−1	410±052E−1	981±122E−1	871±087E−1	108±004E+0
NGC4125	···	138±013E+0	153±015E+0	128±012E+0	641±086E−1	372±050E−1	247±032E−1	143±018E−1	107±010E−1	785±042E−2
NGC4236	···	633±033E−1	829±044E−1	569±034E−1	246±033E−1	185±028E−1	184±014E−1	216±027E−1	143±014E−1	513±055E−1
NGC4254	881±017E−1	126±012E+0	134±013E+0	120±012E+0	700±094E−1	469±064E−1	149±018E+0	393±049E+0	342±034E+0	420±016E+0
NGC4321	126±002E+0	186±018E+0	200±020E+0	164±016E+0	953±128E−1	638±087E−1	121±015E+0	288±035E+0	265±026E+0	333±013E+0
NGC4450	···	120±012E+0	138±013E+0	107±010E+0	529±071E−1	325±044E−1	260±033E−1	268±033E−1	253±025E−1	209±009E−1
NGC4536	501±010E−1	711±071E−1	749±074E−1	698±069E−1	395±053E−1	286±039E−1	620±079E−1	165±020E+0	135±013E+0	346±013E+0
NGC4552	···	162±016E+0	179±017E+0	145±014E+0	828±111E−1	482±066E−1	300±038E−1	170±021E−1	103±010E−1	941±041E−2
NGC4559	558±011E−1	770±077E−1	784±078E−1	655±065E−1	353±048E−1	233±032E−1	421±053E−1	838±104E−1	648±064E−1	111±004E+0
NGC4569	115±002E+0	181±018E+0	207±020E+0	166±016E+0	763±102E−1	473±064E−1	591±075E−1	101±012E+0	961±096E−1	143±005E+0
NGC4579	117±002E+0	203±020E+0	222±022E+0	181±018E+0	867±117E−1	522±071E−1	542±069E−1	729±091E−1	728±072E−1	760±031E−1
NGC4594	556±011E+0	801±040E+0	915±045E+0	754±037E+0	391±053E+0	236±031E+0	180±022E+0	145±016E+0	113±011E+0	773±083E−1
NGC4625	815±018E−2	979±064E−2	113±008E−1	896±088E−2	487±064E−2	307±040E−2	605±076E−2	134±016E−1	115±011E−1	128±013E−1
NGC4631	123±002E+0	174±008E+0	197±010E+0	183±009E+0	119±017E+0	846±115E−1	247±031E+0	584±072E+0	477±047E+0	813±087E+0
NGC4725	161±003E+0	242±024E+0	317±031E+0	240±024E+0	113±015E+0	704±096E−1	753±095E−1	120±015E+0	901±090E−1	859±036E−1
NGC4736	530±010E+0	693±034E+0	766±038E+0	642±032E+0	344±048E+0	229±031E+0	256±034E+0	482±064E+0	467±046E+0	553±059E+0
DDO154	125±005E−2	991±262E−3	124±039E−2	119±047E−2	511±100E−3	350±100E−3	<403E−3	<399E−3	<124E−3	<438E−3
NGC4826	353±007E+0	564±028E+0	628±031E+0	526±026E+0	240±034E+0	151±021E+0	160±021E+0	224±029E+0	191±019E+0	255±027E+0
DDO165	320±009E−2	318±036E−2	468±055E−2	372±062E−2	127±023E−2	909±150E−3	588±170E−3	408±080E−3	<168E−3	<449E−3
NGC5033	···	120±012E+0	134±013E+0	116±011E+0	640±086E−1	470±064E−1	815±103E−1	192±023E+0	177±017E+0	197±007E+0
NGC5055	315±006E+0	420±021E+0	495±024E+0	404±020E+0	237±032E+0	155±021E+0	259±033E+0	558±070E+0	540±054E+0	559±060E+0
NGC5194	300±010E+0	496±024E+0	586±029E+0	451±022E+0	266±036E+0	179±025E+0	423±053E+0	106±013E+1	104±010E+1	124±013E+1

Table 2b—Continued

Galaxy	z	J	H	K_s	IRAC	IRAC	IRAC	IRAC	WISE	MIPS
$\lambda(\mu m)$	0.9097	1.25	1.65	2.17	3.6	4.5	5.8	8.0	12	24
A_λ/A_V	0.4882	0.2964	0.1871	0.1159	0.04514	0.02880	0.01930	0.02962	0.03554	0.01932
NGC5195	149±005E+0	235±011E+0	278±013E+0	225±011E+0	833±113E−1	511±070E−1	462±060E−1	646±080E−1	102±010E+0	146±015E+0
NGC5398	···	805±080E−2	664±066E−2	537±053E−2	377±050E−2	246±036E−2	144±020E−2	587±075E−2	663±066E−2	279±013E−1
NGC5457	391±007E+0	437±022E+0	503±025E+0	441±022E+0	281±038E+0	189±026E+0	339±042E+0	761±094E+0	706±070E+0	105±011E+1
NGC5408	···	185±018E−1	165±016E−1	108±010E−1	514±072E−2	369±051E−2	412±053E−2	377±047E−2	668±066E−2	428±017E−1
NGC5474	225±004E−1	143±009E−1	158±012E−1	113±013E−1	109±013E−1	731±102E−2	555±101E−2	114±014E−1	103±010E−1	156±016E−1
NGC5713	242±004E−1	373±037E−1	386±038E−1	331±033E−1	201±027E−1	137±019E−1	289±037E−1	114±014E+0	101±010E+0	234±009E+0
NGC5866	903±018E−1	130±013E+0	148±014E+0	126±012E+0	663±089E−1	420±057E−1	312±039E−1	314±039E−1	268±026E−1	214±009E−1
IC4710	···	106±010E−1	990±099E−2	772±077E−2	699±097E−2	464±064E−2	450±061E−2	648±083E−2	375±037E−2	118±005E−1
NGC6822	···	552±055E+0	553±055E+0	420±042E+0	210±028E+0	137±018E+0	144±018E+0	140±017E+0	116±011E+0	317±012E+0
NGC6946	···	701±070E+0	531±053E+0	553±055E+0	328±044E+0	217±029E+0	585±073E+0	140±017E+1	135±013E+1	203±008E+1
NGC7331	189±003E+0	282±028E+0	333±033E+0	280±028E+0	160±021E+0	101±014E+0	186±023E+0	404±050E+0	347±034E+0	436±024E+0
NGC7552	···	706±070E−1	796±079E−1	697±069E−1	453±061E−1	360±049E−1	106±013E+0	270±033E+0	273±027E+0	106±004E+1
NGC7793	···	167±008E+0	169±008E+0	130±006E+0	746±104E−1	481±064E−1	104±013E+0	189±023E+0	151±015E+0	209±022E+0

Note. — The compact table entry format TUV±WXYEZ implies (T.UV±W.XY)×10^{Z} in Jy. See § 2 for corrections that have been applied to the data. The uncertainties include both statistical and systematic effects. 5σ upper limits are provided for non-detections. No color corrections have been applied.

Table 2c. Global Flux Densities in Janskys

Galaxy	MIPS	PACS	PACS	MIPS	PACS	SPIRE	SPIRE	SPIRE	SCUBA	VLA
$\lambda(\mu m)$	70	70	100	160	160	250	350	500	850	20 cm
A_λ/A_V	0.002308	0.002308	0.001037	0.000388	0.000388	0.0001521	0.0000725	0.00003605	0.00001458	0.0
NGC0024	222±027E+0	...	...	712±111E+0	...	...	...	...	...	...
NGC0337	111±013E+1	139±006E+1	210±010E+1	200±025E+1	197±009E+1	902±064E+0	409±029E+0	162±011E+0	349±052E−1	109±010E−1
NGC0584	175±498E−1	180±025E−1	300±033E−1	118±050E+0	610±038E−1	<887E−1	<603E−1	<419E−1	...	<500E−2
NGC0628	338±041E+1	421±021E+1	837±041E+1	111±017E+2	114±005E+2	626±044E+1	301±021E+1	116±008E+1	...	172±017E−1
NGC0855	168±020E+0	208±010E+0	253±013E+0	222±034E+0	206±010E+0	137±009E+0	734±053E−1	226±018E−1	...	490±050E−3
NGC0925	143±019E+1	136±006E+1	289±014E+1	433±054E+1	372±018E+1	253±017E+1	139±009E+1	665±047E+0	...	460±050E−2
NGC1097	598±053E+1	787±039E+1	123±006E+2	153±018E+2	132±006E+2	674±047E+1	296±021E+1	109±007E+1	144±078E+0	414±041E−1
NGC1266	126±015E+1	149±007E+1	171±008E+1	102±014E+1	113±005E+1	408±029E+0	147±010E+0	410±031E−1	...	116±012E−1
NGC1291	527±064E+0	439±027E+0	135±007E+1	262±041E+1	226±011E+1	152±010E+1	766±054E+0	316±022E+0	...	...
NGC1316	544±126E+0	568±029E+0	997±050E+0	126±019E+1	124±006E+1	499±035E+0	206±015E+0	721±059E−1	...	255±026E−1
NGC1377	634±095E+0	725±036E+0	651±032E+0	338±056E+0	337±016E+0	123±008E+0	474±034E−1	167±013E−1	...	<100E−3
NGC1404	<165E−1	<214E−1	<252E−1	<286E−1	<204E−1	<163E−1	<134E−1	<909E−2	...	390±060E−3
IC0342	352±024E+2	471±023E+2	895±044E+2	915±109E+2	107±005E+3	569±040E+2	254±018E+2	941±066E+1	...	240±024E+0
NGC1482	324±034E+1	419±020E+1	522±026E+1	387±048E+1	419±021E+1	155±011E+1	588±041E+0	180±012E+0	330±050E−1	238±024E−1
NGC1512	682±083E+0	752±039E+0	150±007E+1	196±030E+1	191±009E+1	148±010E+1	875±062E+0	371±027E+0	...	700±100E−3
NGC1566	343±032E+1	...	...	102±012E+2	...	...	...	...	...	400±000E−1
NGC1705	124±015E+0	...	...	139±021E+0	...	...	...	...	...	...
NGC2146	215±015E+2	198±009E+2	236±011E+2	119±014E+2	174±008E+2	618±043E+1	223±015E+1	695±049E+0	...	107±010E+0
NGC2403	857±104E+1	...	...	225±035E+2	...	...	...	...	...	330±033E−1
HoII	318±039E+0	438±022E+0	574±028E+0	346±054E+0	363±018E+0	154±011E+0	779±067E−1	289±144E−1	...	197±028E−2
M81dwA	<149E−1	...	...	<143E−1	...	...	...	...	...	...
DDO053	315±040E−1	400±025E−1	520±031E−1	357±061E−1	300±020E−1	140±014E−1	100±010E−1	<389E−2	...	...
NGC2798	217±023E+1	250±012E+1	287±014E+1	206±026E+1	202±010E+1	746±053E+0	275±019E+0	870±062E−1	194±032E−1	829±085E−2
NGC2841	102±014E+1	110±005E+1	286±014E+1	622±076E+1	488±024E+1	324±023E+1	154±010E+1	600±042E+0	...	840±086E−2
NGC2915	140±047E+0	107±005E+0	180±009E+0	145±041E+0	162±008E+0	823±059E−1	468±034E−1	209±016E−1	...	...
HoI	292±040E−1	401±033E−1	441±039E−1	526±092E−1	432±034E−1	372±031E−1	231±020E−1	110±012E−1	...	...
NGC2976	199±024E+1	209±010E+1	372±018E+1	426±066E+1	459±022E+1	244±017E+1	114±008E+1	451±032E+0	609±236E−1	508±054E−2
NGC3049	289±072E+0	382±019E+0	529±026E+0	486±072E+0	494±024E+0	261±018E+0	132±009E+0	657±047E−1	...	120±023E−2
NGC3031	852±104E+1	...	...	308±048E+2	...	...	...	...	...	379±037E−1
NGC3034	162±051E+3	...	...	857±271E+2	...	...	...	...	551±082E+0	765±077E+0
HoIX	<228E−1	...	...	<457E−1	...	...	...	...	...	...
NGC3077	196±024E+1	213±010E+1	293±014E+1	281±043E+1	278±013E+1	133±009E+1	620±044E+0	242±017E+0	...	...
M81dwB	114±016E−1	904±116E−2	270±018E−1	161±031E−1	292±018E−1	178±014E−1	105±010E−1	435±217E−2	...	...

Table 2c—Continued

Galaxy	MIPS	PACS	PACS	MIPS	PACS	SPIRE	SPIRE	SPIRE	SCUBA	VLA
$\lambda(\mu m)$	70	70	100	160	160	250	350	500	850	20 cm
A_λ/A_V	0.002308	0.002308	0.001037	0.000388	0.000388	0.0001521	0.0000725	0.00003605	0.00001458	0.0
NGC3190	565±094E+0	629±031E+0	109±005E+1	150±019E+1	153±007E+1	826±058E+0	352±025E+0	121±008E+0	189±035E−1	430±047E−2
NGC3184	157±020E+1	180±009E+1	392±019E+1	704±086E+1	537±026E+1	317±022E+1	148±010E+1	589±042E+0	···	559±059E−2
NGC3198	102±013E+1	109±005E+1	224±011E+1	389±050E+1	296±014E+1	183±013E+1	965±068E+0	412±029E+0	···	270±034E−2
IC2574	483±059E+0	578±029E+0	937±047E+0	105±016E+1	986±049E+0	574±041E+0	417±029E+0	169±012E+0	···	107±023E−2
NGC3265	270±066E+0	292±014E+0	322±016E+0	270±047E+0	285±014E+0	116±008E+0	514±037E−1	198±016E−1	···	111±023E−2
Mrk33	434±081E+0	···	···	386±060E+0	···	···	···	···	400±060E−2	172±026E−2
NGC3351	218±026E+1	270±013E+1	486±024E+1	569±088E+1	538±026E+1	316±022E+1	139±009E+1	490±034E+0	···	438±048E−2
NGC3521	644±078E+1	800±040E+1	163±008E+2	195±030E+2	203±010E+2	107±007E+2	464±032E+1	168±011E+1	210±082E+0	356±035E−1
NGC3621	501±046E+1	504±025E+1	101±005E+2	139±017E+2	124±006E+2	654±046E+1	308±021E+1	125±008E+1	···	197±019E−1
NGC3627	919±070E+1	107±005E+2	188±009E+2	215±027E+2	196±009E+2	912±064E+1	364±025E+1	123±008E+1	186±070E+0	457±045E−1
NGC3773	157±052E+0	139±007E+0	214±010E+0	238±048E+0	206±010E+0	953±068E−1	419±030E−1	158±012E−1	···	580±050E−3
NGC3938	142±017E+1	164±008E+1	307±015E+1	519±063E+1	392±019E+1	221±015E+1	993±070E+0	373±026E+0	···	617±065E−2
NGC4125	111±052E+0	···	···	176±042E+0	···	···	···	···	···	<500E−2
NGC4236	802±098E+0	803±041E+0	113±005E+1	161±025E+1	172±008E+1	107±007E+1	702±050E+0	364±026E+0	···	281±034E−2
NGC4254	502±043E+1	596±029E+1	110±005E+2	142±017E+2	126±006E+2	623±044E+1	252±017E+1	849±060E+0	100±054E+0	421±041E−1
NGC4321	405±037E+1	440±022E+1	907±045E+1	139±016E+2	116±005E+2	632±044E+1	268±019E+1	919±065E+0	875±493E−1	340±034E−1
NGC4450	342±108E+0	···	···	169±022E+1	···	···	···	···	···	940±100E−3
NGC4536	319±031E+1	419±020E+1	567±028E+1	580±071E+1	555±027E+1	270±019E+1	122±008E+1	471±033E+0	414±112E−1	194±018E−1
NGC4552	537±778E−1	···	···	142±073E+0	···	···	···	···	···	100±003E−1
NGC4559	168±019E+1	180±009E+1	337±016E+1	541±066E+1	405±020E+1	238±016E+1	123±008E+1	540±038E+0	···	654±068E−2
NGC4569	123±015E+1	148±007E+1	325±016E+1	412±052E+1	400±020E+1	210±014E+1	909±064E+0	315±022E+0	464±082E−1	834±086E−2
NGC4579	953±140E+0	100±005E+1	254±012E+1	410±050E+1	345±017E+1	196±013E+1	852±060E+0	303±021E+0	439±066E−1	984±100E−2
NGC4594	730±089E+0	808±041E+0	259±013E+1	406±063E+1	380±019E+1	240±017E+1	117±008E+1	487±034E+0	372±108E−1	136±014E−1
NGC4625	185±022E+0	151±008E+0	376±019E+0	508±079E+0	469±023E+0	258±018E+0	131±009E+0	560±041E−1	···	710±210E−3
NGC4631	138±016E+2	140±007E+2	233±011E+2	269±042E+2	238±011E+2	115±008E+2	529±037E+1	205±014E+1	573±120E+0	120±012E+0
NGC4725	885±140E+0	103±005E+1	260±013E+1	599±074E+1	466±023E+1	305±021E+1	162±011E+1	661±047E+0	···	280±034E−2
NGC4736	100±012E+2	107±005E+2	165±008E+2	164±025E+2	141±007E+2	640±045E+1	263±018E+1	920±065E+0	153±065E+0	270±027E−1
DDO154	<591E−2	<775E−2	<912E−2	<223E−1	<801E−2	<544E−2	<483E−2	<349E−2	···	···
NGC4826	528±064E+1	563±028E+1	975±048E+1	857±133E+1	906±045E+1	396±028E+1	158±011E+1	527±037E+0	123±030E+0	101±009E−1
DDO165	<141E−1	<976E−2	<119E−1	<205E−1	<101E−1	<807E−2	<713E−2	<484E−2	···	···
NGC5033	288±028E+1	···	···	910±112E+1	···	···	···	···	109±055E+0	178±017E−1
NGC5055	744±090E+1	764±038E+1	175±008E+2	273±042E+2	241±012E+2	139±009E+2	617±043E+1	225±016E+1	···	389±039E−1
NGC5194	156±019E+2	···	···	477±074E+2	···	···	···	···	261±039E+0	149±015E+0

Table 2c—Continued

Galaxy	MIPS	PACS	PACS	MIPS	PACS	SPIRE	SPIRE	SPIRE	SCUBA	VLA
$\lambda(\mu m)$	70	70	100	160	160	250	350	500	850	20 cm
A_λ/A_V	0.002308	0.002308	0.001037	0.000388	0.000388	0.0001521	0.0000725	0.00003605	0.00001458	0.0
NGC5195	972±118E+0	···	···	129±020E+1	···	···	···	···	259±039E−1	495±053E−2
NGC5398	203±059E+0	245±012E+0	333±016E+0	351±065E+0	283±014E+0	188±013E+0	102±007E+0	499±036E−1	···	420±080E−3
NGC5457	118±014E+2	135±006E+2	262±013E+2	399±062E+2	336±016E+2	195±013E+2	952±067E+1	396±028E+1	···	749±075E−1
NGC5408	358±075E+0	369±018E+0	275±014E+0	256±052E+0	231±011E+0	829±061E−1	420±032E−1	150±014E−1	···	···
NGC5474	347±042E+0	354±018E+0	604±031E+0	913±142E+0	853±043E+0	486±034E+0	283±020E+0	136±009E+0	···	120±023E−2
NGC5713	236±024E+1	295±014E+1	421±021E+1	396±049E+1	385±019E+1	157±011E+1	615±043E+0	197±014E+0	572±119E−1	159±016E−1
NGC5866	870±120E+0	880±044E+0	180±009E+1	177±022E+1	178±008E+1	764±054E+0	308±022E+0	984±073E−1	140±020E−1	227±030E−2
IC4710	237±074E+0	···	···	356±065E+0	···	···	···	···	···	···
NGC6822	637±061E+1	···	···	143±017E+2	···	···	···	···	···	694±140E−2
NGC6946	207±016E+2	252±012E+2	457±022E+2	502±060E+2	525±026E+2	258±018E+2	107±007E+2	369±026E+1	298±044E+0	139±014E+0
NGC7331	749±073E+1	688±034E+1	135±006E+2	189±024E+2	171±008E+2	890±063E+1	389±027E+1	142±010E+1	211±038E+0	372±037E−1
NGC7552	675±114E+1	···	···	933±113E+1	···	···	···	···	795±166E−1	275±028E−1
NGC7793	329±040E+1	350±017E+1	695±034E+1	107±016E+2	901±045E+1	531±037E+1	279±019E+1	120±008E+1	···	102±009E−1

Note. — The compact table entry format TUV±WXYEZ implies (T.UV±W.XY)$\times 10^{\mathrm{Z}}$ in Jy. See § 2 for corrections that have been applied to the data. The uncertainties include both statistical and systematic effects. 5σ upper limits are provided for non-detections. No color corrections have been applied.

Table 3. Optical $BVR_{\rm C}I_{\rm C}$ Photometry Source

Galaxy	B	V	$R_{\rm C}$	$I_{\rm C}$
NGC0024	PS1	PS1	PS1	PS1
NGC0337	PS1	PS1	PS1	PS1
NGC0584	PS1	PS1	PS1	PS1
NGC0628	PS1	PS1	PS1	PS1
NGC0855	RC3	RC3	C14	···
NGC0925	PS1	PS1	PS1	PS1
NGC1097	MM09	MM09	MM09	MM09
NGC1266	PS1	PS1	PS1	PS1
NGC1291	MM09	MM09	MM09	MM09
NGC1316	MM09	MM09	MM09	MM09
NGC1377	PS1	PS1	PS1	PS1
NGC1404	MM09	MM09	MM09	MM09
IC0342	RC3	···	···	···
NGC1482	PS1	PS1	PS1	PS1
NGC1512	MM09	MM09	MM09	MM09
NGC1566	MM09	MM09	MM09	MM09
NGC1705	MM09	MM09	MM09	MM09
NGC2403	PS1	PS1	PS1	PS1
NGC2146	RC3	RC3	···	T09
HolmbII	PS1	PS1	PS1	PS1
M81dwA	PS1	PS1	PS1	PS1
DDO053	PS1	PS1	PS1	PS1
NGC2798	PS1	PS1	PS1	PS1
NGC2841	PS1	PS1	PS1	PS1
NGC2915	RC3	MM09	MM09	D07
HolmbI	PS1	PS1	PS1	PS1
NGC2976	PS1	PS1	PS1	PS1
NGC3049	PS1	PS1	PS1	PS1
NGC3031	RC3	RC3	···	T09
NGC3034	PS1	PS1	PS1	PS1
HolmbIX	PS1	PS1	PS1	PS1
NGC3077	C14	···	RC3	···
M81dwB	PS1	PS1	PS1	PS1
NGC3190	PS1	PS1	PS1	PS1
NGC3184	PS1	PS1	PS1	PS1
NGC3198	PS1	PS1	PS1	PS1
IC2574	PS1	PS1	PS1	PS1
NGC3265	PS1	PS1	PS1	PS1
Mrk33	PS1	PS1	PS1	PS1
NGC3351	PS1	PS1	PS1	PS1
NGC3521	PS1	PS1	PS1	PS1
NGC3621	MM09	MM09	MM09	MM09
NGC3627	PS1	PS1	PS1	PS1
NGC3773	PS1	PS1	PS1	PS1
NGC3938	PS1	PS1	PS1	PS1
NGC4125	PS1	PS1	PS1	PS1

Table 3—Continued

Galaxy	B	V	R_C	I_C
NGC4236	PS1	PS1	PS1	PS1
NGC4254	PS1	PS1	PS1	PS1
NGC4321	PS1	PS1	PS1	PS1
NGC4450	PS1	PS1	PS1	PS1
NGC4536	PS1	PS1	PS1	PS1
NGC4552	PS1	PS1	PS1	PS1
NGC4559	PS1	PS1	PS1	PS1
NGC4569	RC3	RC3	···	···
NGC4579	PS1	PS1	PS1	PS1
NGC4594	PS1	PS1	PS1	PS1
NGC4625	PS1	PS1	PS1	PS1
NGC4631	PS1	PS1	PS1	PS1
NGC4725	PS1	PS1	PS1	PS1
NGC4736	PS1	PS1	PS1	PS1
DDO154	PS1	PS1	PS1	PS1
NGC4826	PS1	PS1	PS1	PS1
DDO165	PS1	PS1	PS1	PS1
NGC5033	PS1	PS1	···	PS1
NGC5055	RC3	RC3	C14	T09
NGC5194	PS1	PS1	PS1	PS1
NGC5195	PS1	PS1	PS1	PS1
NGC5398	D07	D07	D07	D07
NGC5457	RC3	RC3	C14	T09
NGC5408	RC3	RC3	···	···
NGC5474	PS1	PS1	PS1	PS1
NGC5713	PS1	PS1	PS1	PS1
NGC5866	PS1	PS1	PS1	PS1
IC4710	D07	D07	D07	···
NGC6822	PS1	PS1	PS1	PS1
NGC6946	RC3	PS1	···	PS1
NGC7331	PS1	PS1	PS1	PS1
NGC7552	MM09	MM09	D07	D07
NGC7793	D07	D07	D07	D07

Note. — PS1: recalibration of Dale et al. (2007) photometry using Pan-STARRS1 (§2.1); D07: Dale et al. (2007); MM09: Muñoz-Mateos et al. (2009); C14: Cook et al. (2014); T09: unpublished photometry from M. Pierce via the Extragalactic Distance Database (Tully et al. 2009); RC3: de Vaucouleurs et al. (1991).

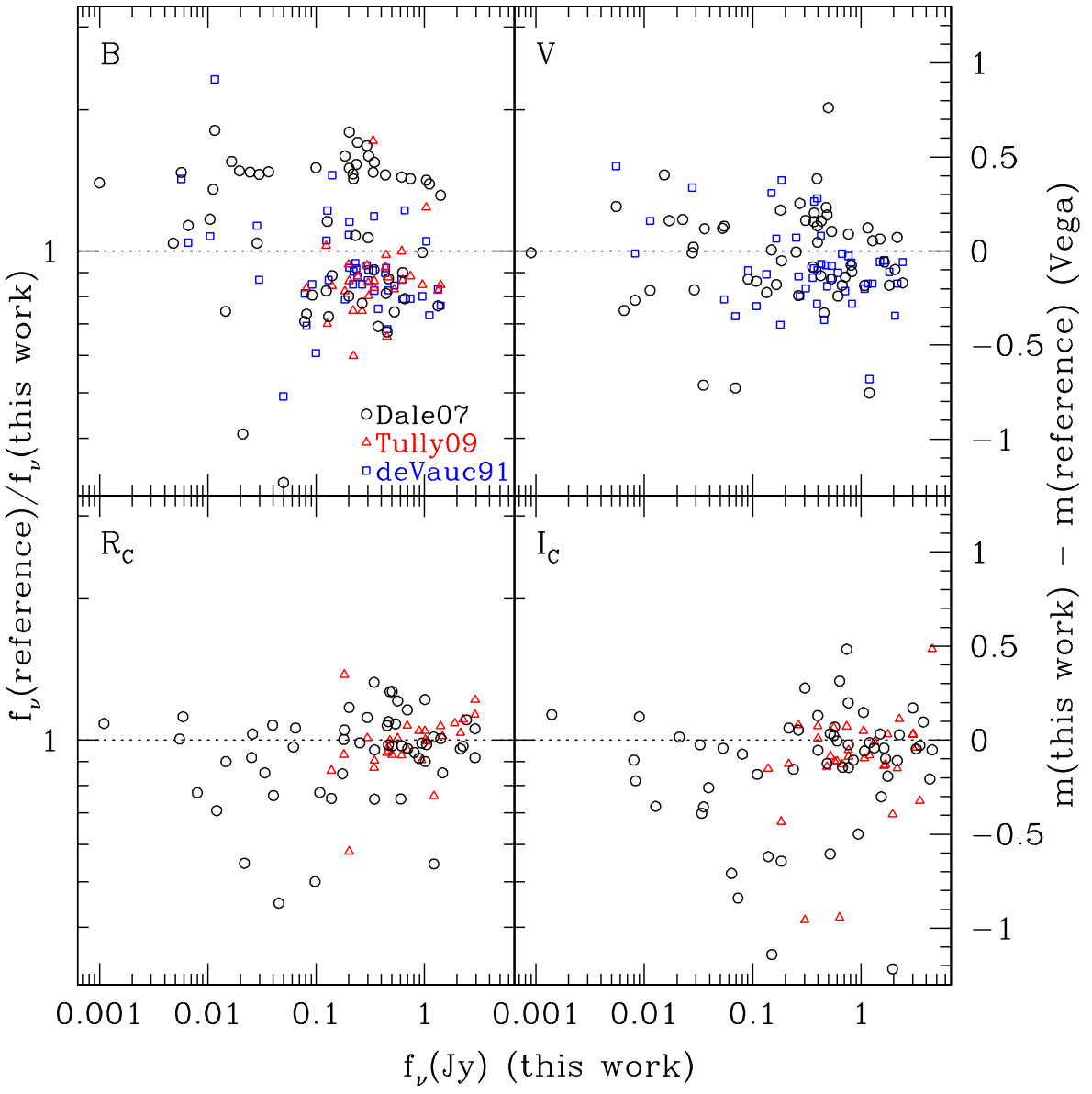

Fig. 1.— Comparison of global $BVR_{\rm C}I_{\rm C}$ photometry from the literature with those measured here which are calibrated based on Pan-STARRS1 $g_{\rm P1}r_{\rm P1}i_{\rm P1}z_{\rm P1}$ photometry on field stars (see § 2.1).

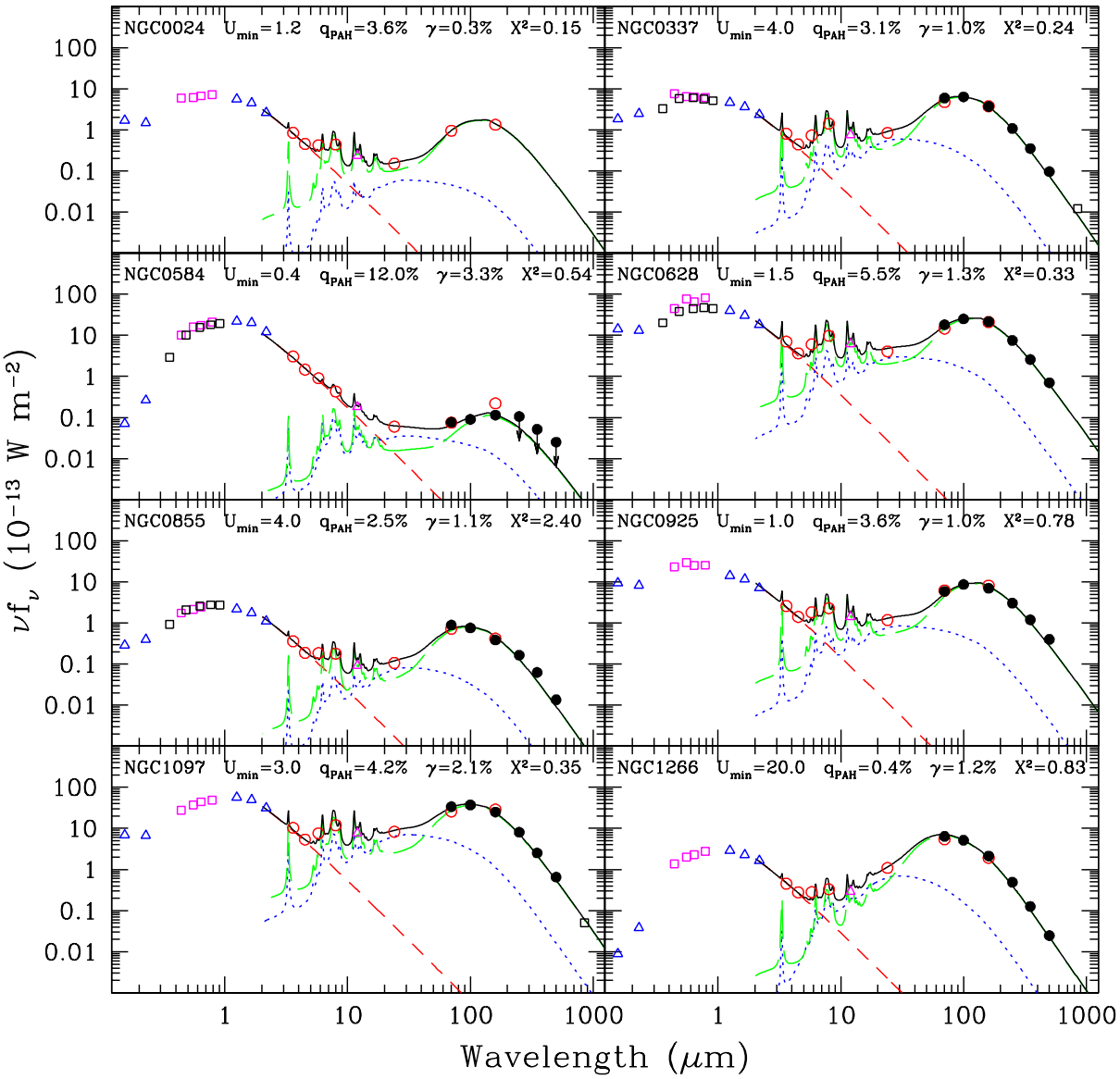

Fig. 2.— Globally-integrated infrared/sub-millimeter spectral energy distributions for all the galaxies in the KINGFISH sample, sorted by Right Ascension. Herschel data are represented by filled circles and ancillary data are indicated by open symbols (triangles: *2MASS* and *IRAS*; circles: *Spitzer*; squares: *ISO* and SCUBA); stars: *WISE*. Arrows indicate 5σ upper limits. The solid curve is the sum of a 5000 K stellar blackbody (short dashed) along with models of dust emission from PDRs (dotted; $U > U_{\rm min}$) and the diffuse interstellar medium (long dashed; $U = U_{\rm min}$). The fitted parameters from these **?** model fits are listed within each panel along with the reduced χ^2 (see § 3.4 for details).

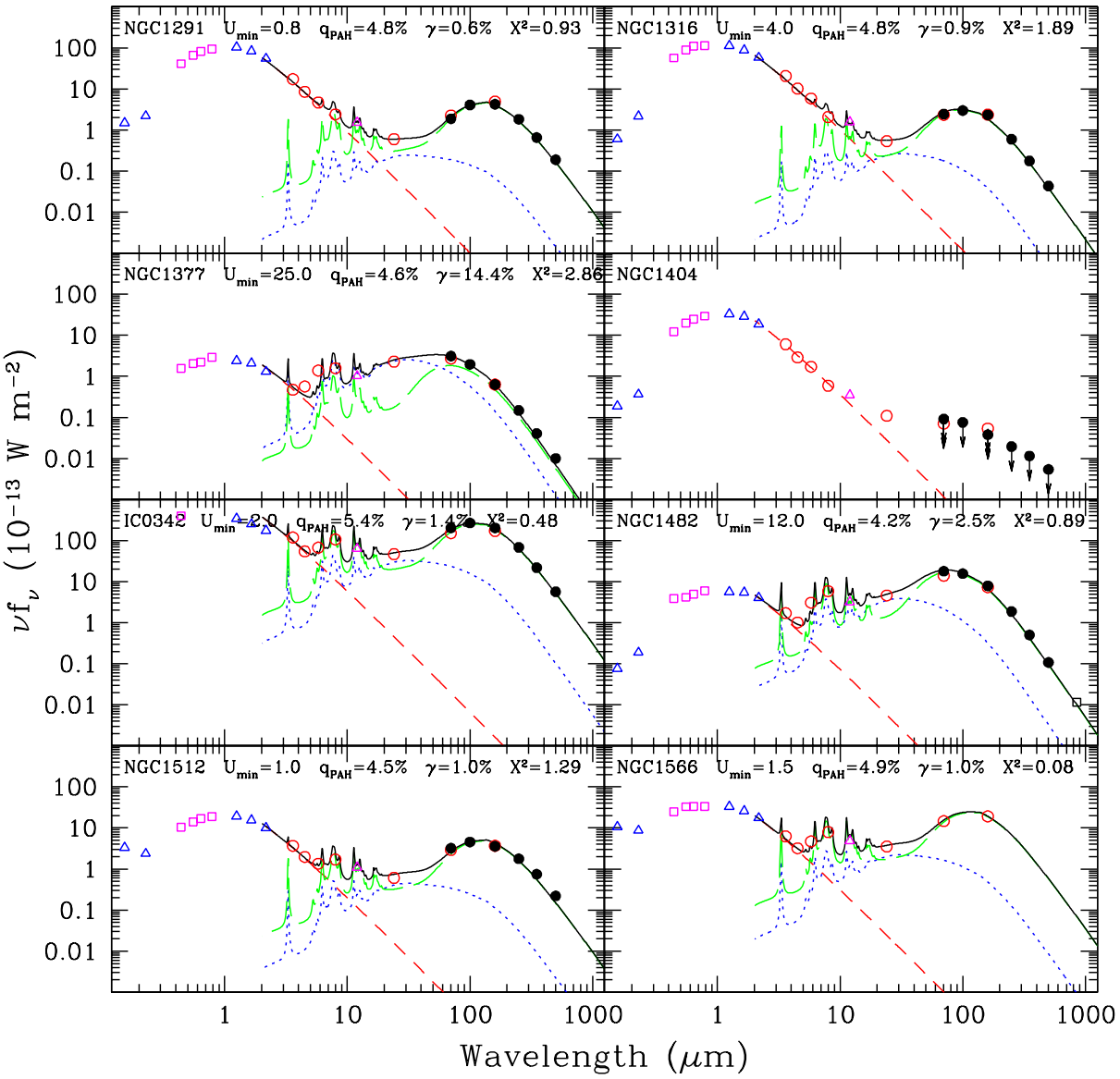

Fig. 2.— Globally-integrated infrared/sub-millimeter spectral energy distributions for the KINGFISH sample (continued).

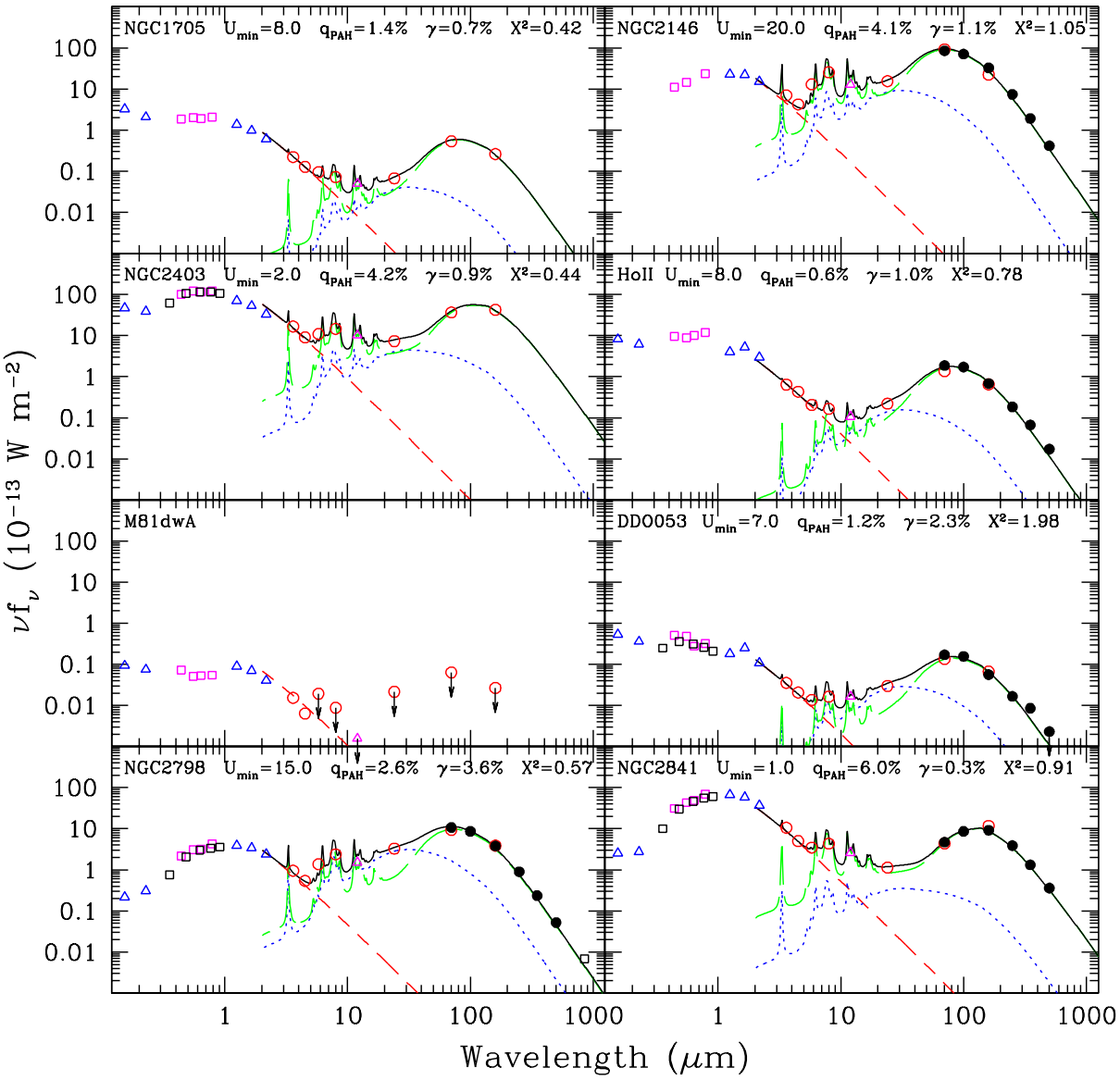

Fig. 2.— Globally-integrated infrared/sub-millimeter spectral energy distributions for the KINGFISH sample (continued).

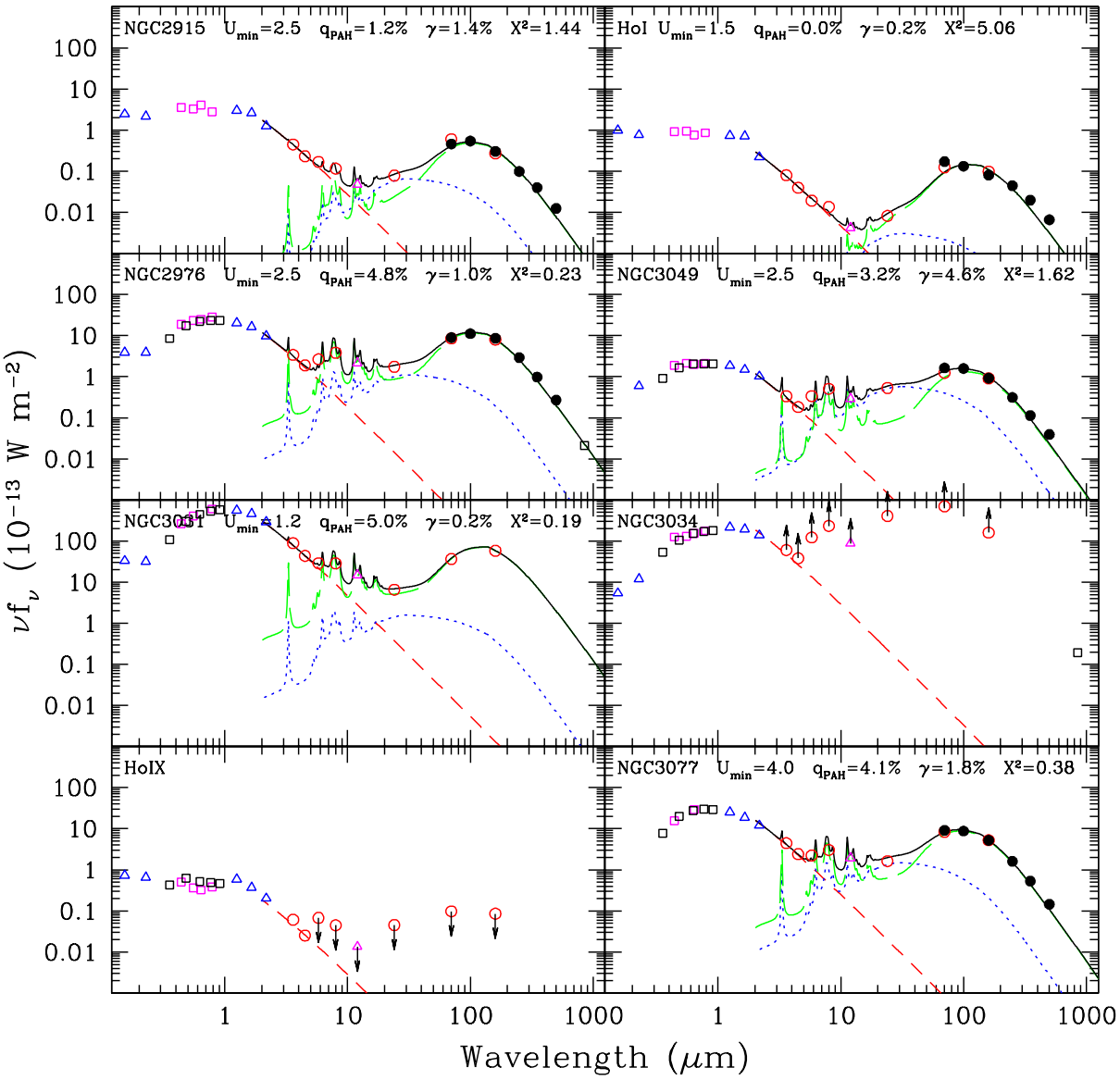

Fig. 2.— Globally-integrated infrared/sub-millimeter spectral energy distributions for the KINGFISH sample (continued).

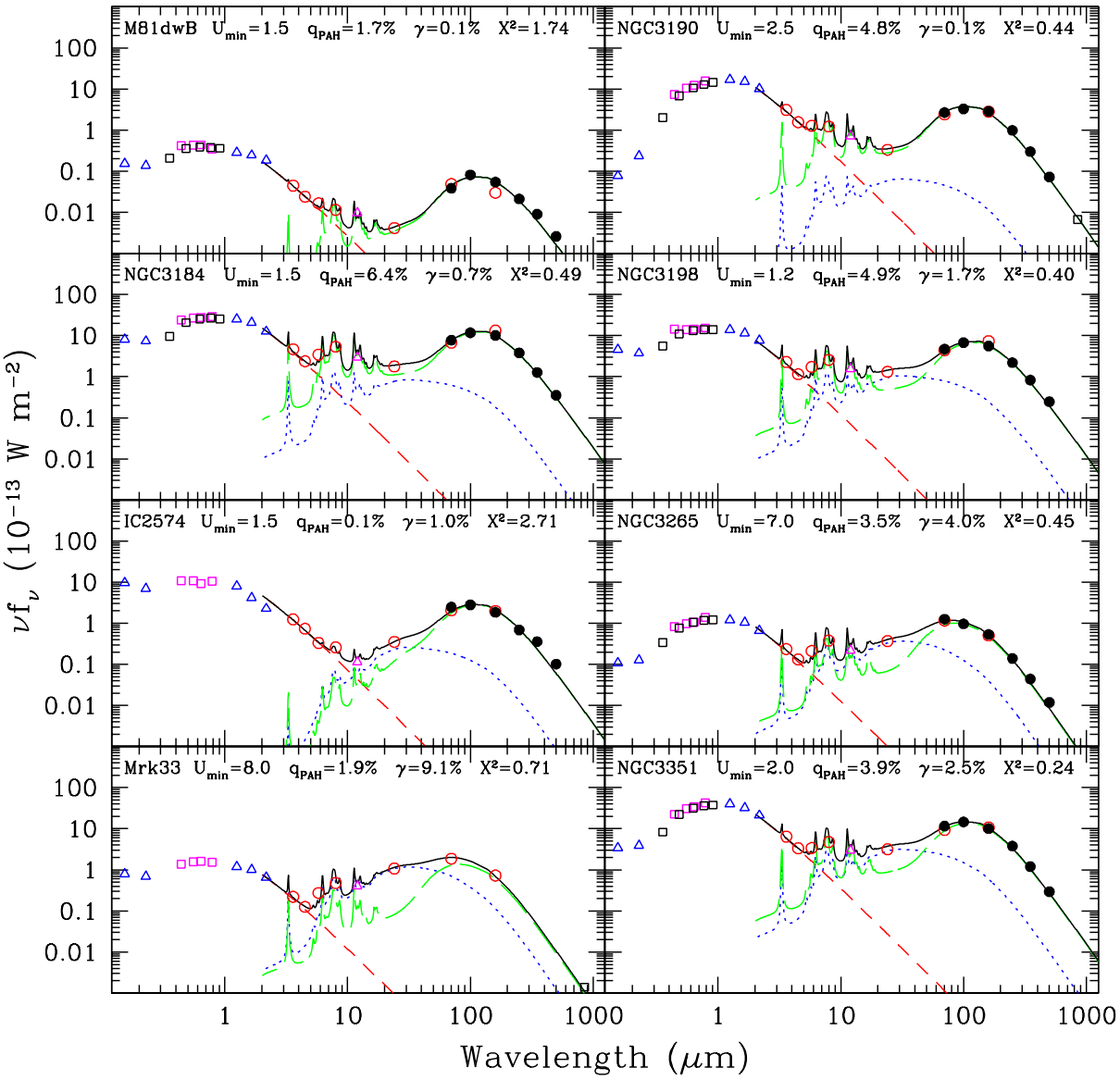

Fig. 2.— Globally-integrated infrared/sub-millimeter spectral energy distributions for the KINGFISH sample (continued).

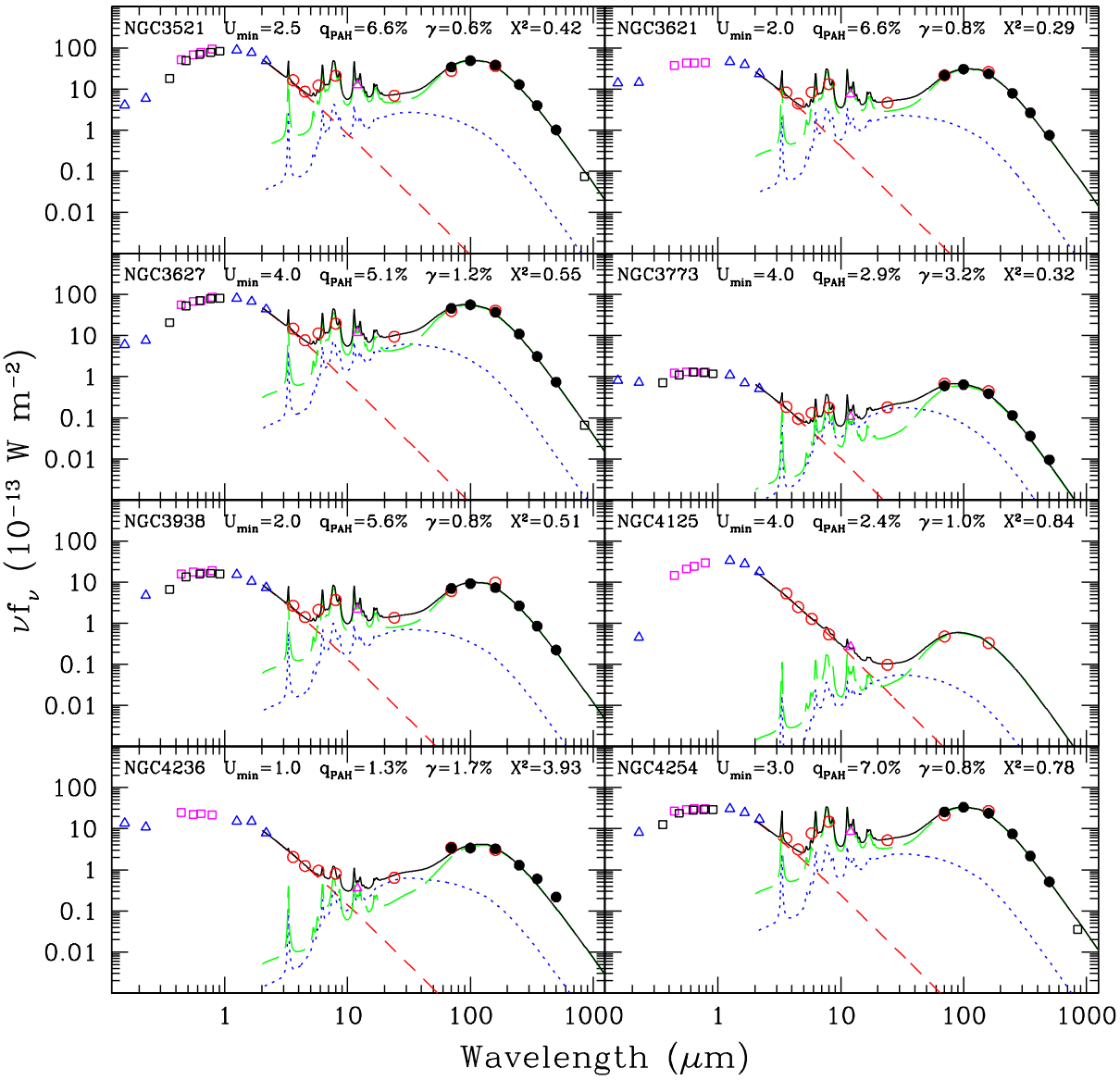

Fig. 2.— Globally-integrated infrared/sub-millimeter spectral energy distributions for the KINGFISH sample (continued).

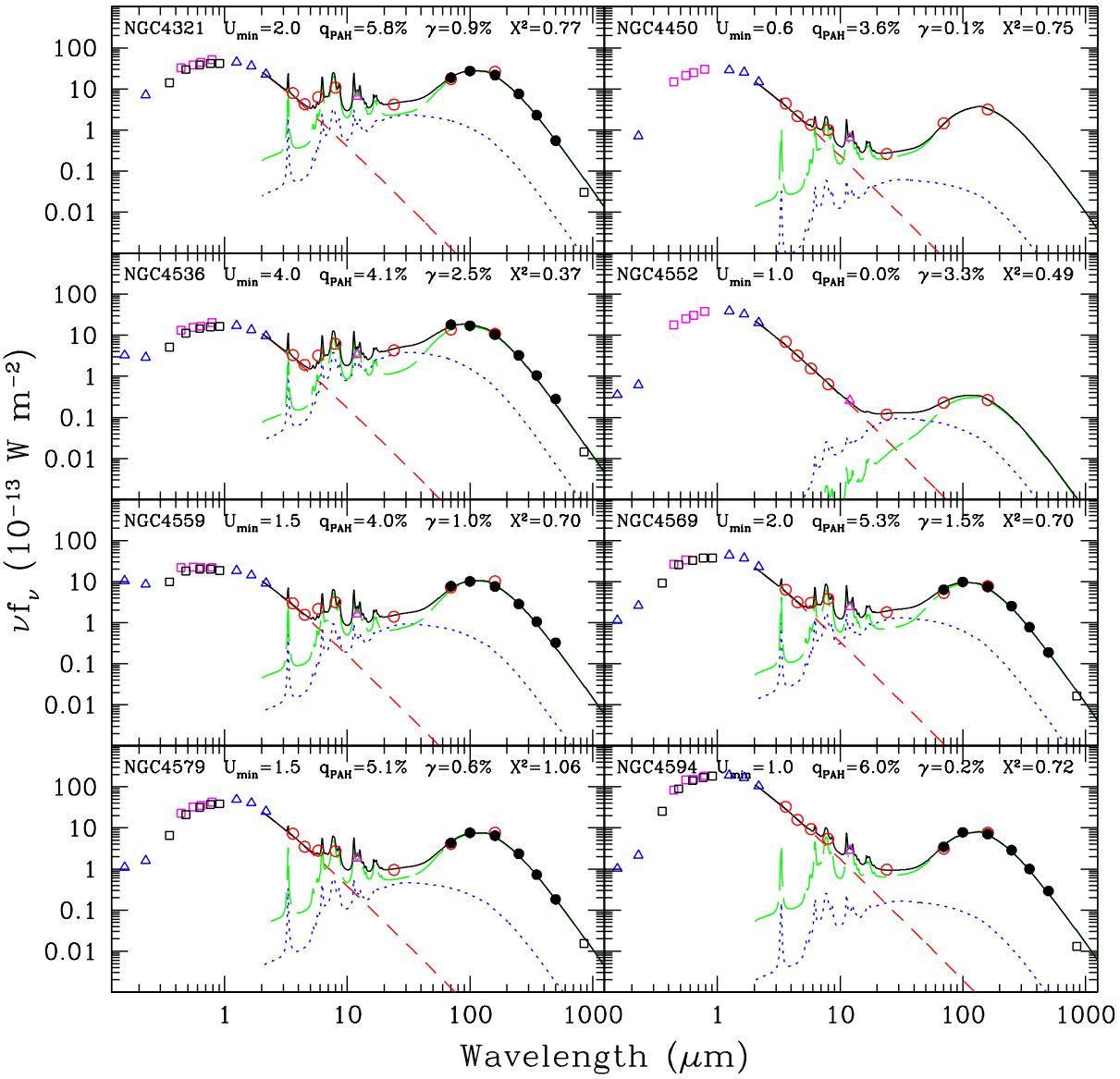

Fig. 2.— Globally-integrated infrared/sub-millimeter spectral energy distributions for the KINGFISH sample (continued).

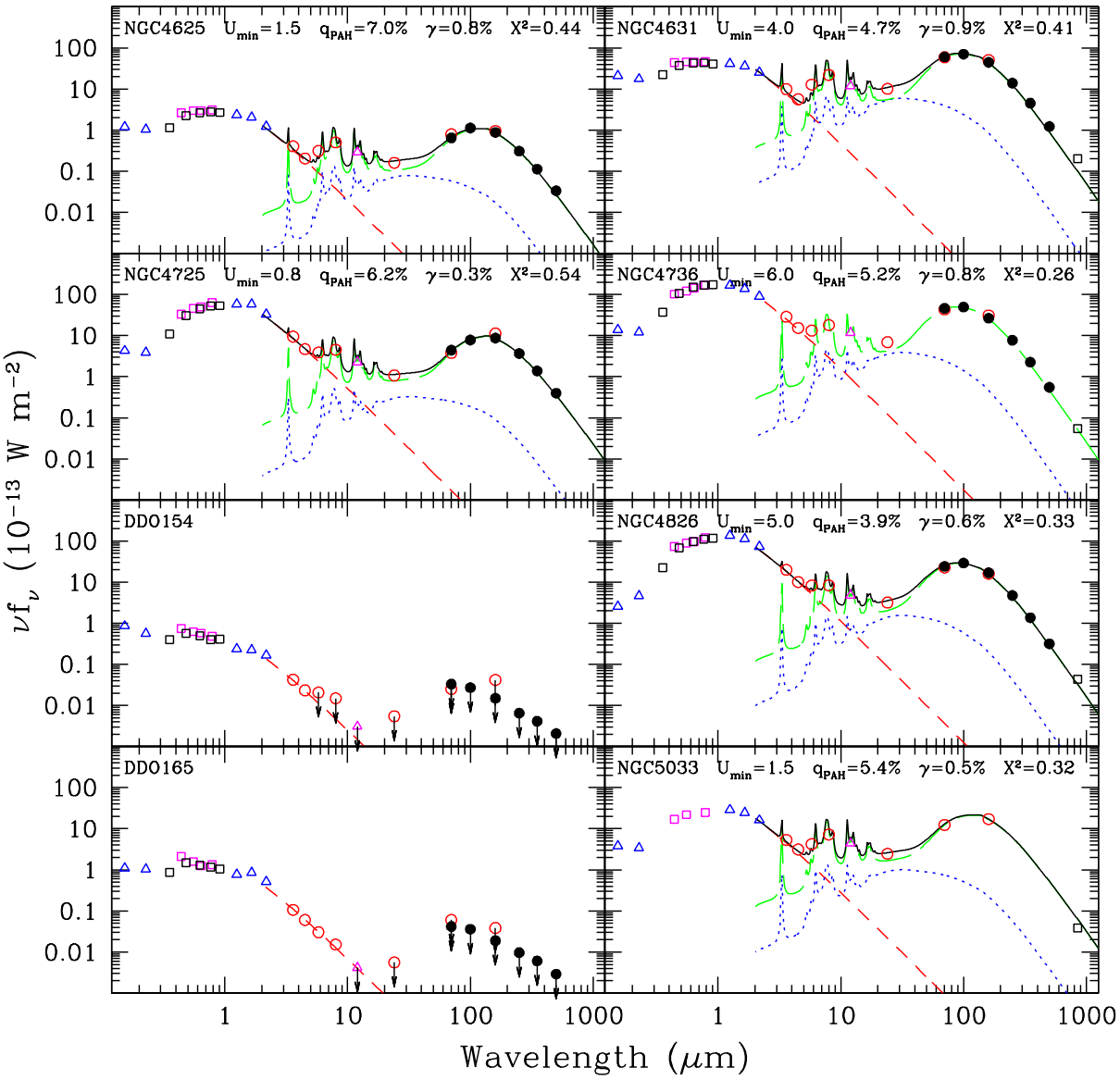

Fig. 2.— Globally-integrated infrared/sub-millimeter spectral energy distributions for the KINGFISH sample (continued).

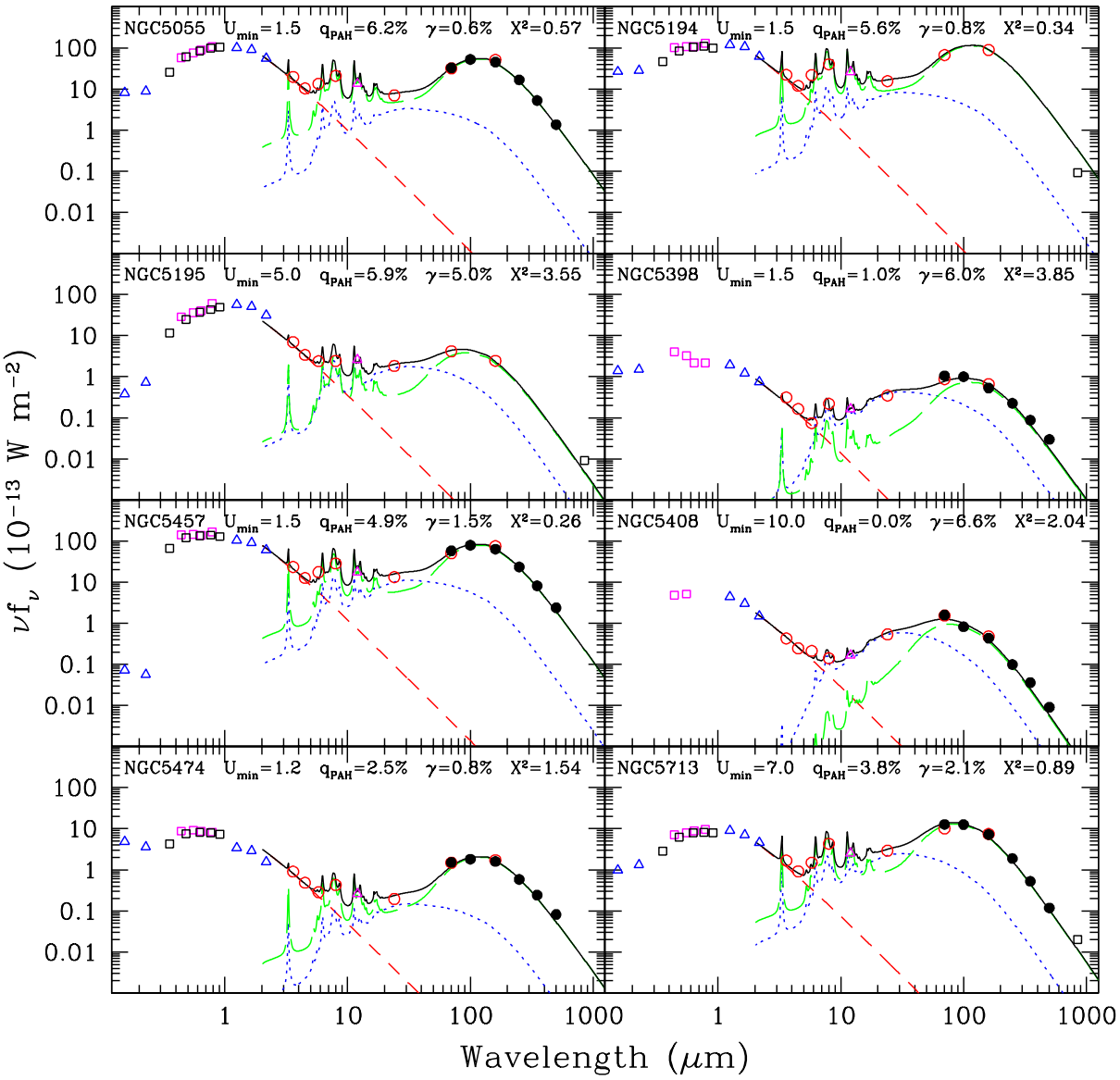

Fig. 2.— Globally-integrated infrared/sub-millimeter spectral energy distributions for the KINGFISH sample (continued).

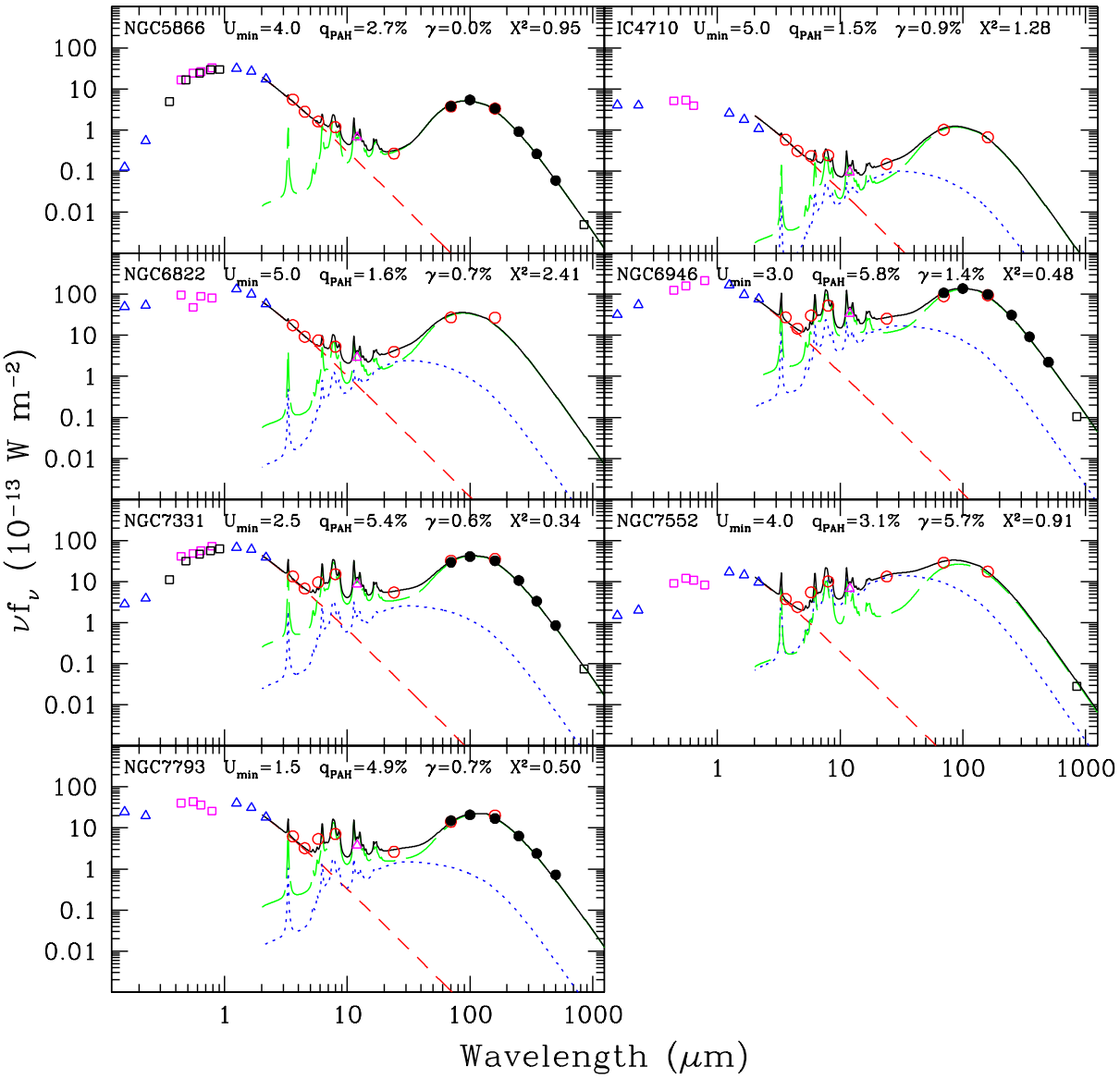

Fig. 2.— Globally-integrated infrared/sub-millimeter spectral energy distributions for the KINGFISH sample (continued).